JPE 14-1-18

http://dx.doi.org/10.6113/JPE.2014.14.1.175
ISSN(Print): 1598-2092 / ISSN(Online): 2093-4718

A PI Control Algorithm with Zero Static Misadjustment for Tracking the Harmonic Current of Three-Level APFs

Yingjie He†, Jinjun Liu*, Zhaoan Wang*, and Yunping Zou**

†*State Key Laboratory of Electrical Insulation and Power Equipment, Xi'an Jiaotong University, Xi'an, China
**Dept. of Electrical and Electronic Eng., Huazhong University of Science & Technology, Wuhan, China

Abstract

Tracking harmonic current quickly and precisely is one of the keys to designing active power filters (APF). In the past, the current state feedback decoupling PI control was an effective means for three-phase systems in the current control of constant voltage constant frequency inverters and high frequency PWM reversible rectifiers. This paper analyzes in detail the limitation of the conventional PI conditioner in the APF application field and presents a novel PI control method. Canceling the delay of one sampling period and the misadjustment for tracking the harmonic current is the key problem of this PI control. In this PI control, the predictive output current value is obtained by a state observer. The delay of one sampling period is remedied in this digital control system by the state observer. The predictive harmonic command current value is obtained by a repetitive predictor synchronously. The repetitive predictor can achieve better predictions of the harmonic current. By this means, the misadjustment of the conventional PI control for tracking the harmonic current is cancelled. The experiment results with a three-level NPC APF indicate that the steady-state accuracy and dynamic response of this method are satisfying when the proposed control scheme is implemented.

Key words: Active power filter, PI control, Repetitive predictor, State observer, Three-level NPC inverter

I. INTRODUCTION

Harmonics cause serious problems for power conversion systems. Passive filters that consist of *L* and ***C*** are generally implemented to attenuate the harmonics generated in the power system. However, passive filters have disadvantages in that the source impedance affects the filtering characteristics and amplification of the harmonic currents caused by the parallel resonance. The control of harmonic perturbations by active power filters (APF) has become a hot topic in the power engineering field. In the past two decades, active power filters have been developed rapidly to suppress the harmonics in power distribution systems of 380V grids [1]-[4]. However, the voltage grids are 600V in many power distribution systems for making petroleum holes. 690V grids are widely used in many of the power distribution systems of mining. There are many voltage grids ranging from 600V to 1000V in steel-making factories. Due to the limitations of the voltage and current capabilities of power devices, it is very difficult to handle the nonlinear loads in the above mentioned voltage grids with the traditional APFs of a 380V grid with a two-level inverter. In recent years, three-level neutral-point-clamped (NPC) PWM inverters have become an effective and practical solution for many moderate voltage application fields [5]. Evidently, the three-level inverter is very suitable for the harmonic restriction of the above mentioned voltage grids. By adopting this topology, a three-level APF with a 1200V IGBT may be used directly in 600V and 690V voltage grids, and a three-level APF with a 1700V IGBT can be applied directly to 1000V voltage grids. Moreover, this topology can synthesize more output levels which is good for harmonic current tracking. In addition, the three-level inverter can be combined with a passive filter to form the hybrid filter used in 6.6kV grids. The hybrid filter can use a 1200V IGBT at a reasonable cost from the market [6], [7]. The APFs with a

Manuscript received Apr. 24, 2013; accepted Oct. 13, 2013
Recommended for publication by Associate Editor Marian P. Kazmierkowski.
†Corresponding Author: yjhe@mail.xjtu.edu.cn
Tel: +86-29-82668666, Fax: +86-29-82668253,Xi'an Jiaotong University
*State Key Laboratory of Electrical Insulation and Power Equipment, Xi'an Jiaotong University, China
**Dept. of Electrical and Electronic Eng., Huazhong University of Science & Technology, China

three-level NPC inverter have received more and more attention in recent years [6]-[12].

The high quality system current waveforms of a power system evaluated with little total harmonic distortion (THD) are a basic requirement for APFs [13]-[21]. Among them, the current state feedback decoupling PI control is distinguished by its simple structure and fast response while this control scheme provides lower current ripples and a constant switching frequency. It is widely applied in the current waveform control of three-phase inverters, PWM rectifiers, STATCOMs and motor drives with sinusoidal inputs or outputs [13]-[18]. However, when this control is applied to an APF, there are some new problems that need to be solved. Firstly, the PI controller may track the DC signal with zero steady-state error. When the fundamental signal is converted into a DC quantity through synchronous rotating transformation in three-phase inverters, STATCOMs and PWM rectifiers, the conventional PI controller may track the command signal in the rotating *dq* frame with zero steady-state error. However, the command current of the APF includes a large number of harmonics. The bandwidth of the conventional PI controller is almost enough for effectively tracking the command harmonic current. As a result, the conventional PI controller will have a large tracking error and the system current waveform filtered has a large THD. How to eliminate the tracking error?

The execution of the control program needs time. The calculation of the command voltage should be carried out a sampling period ahead, otherwise the maximum output pulse width will be significantly reduced. Under most conditions, the calculation of the command voltage in this sampling period will be carried out in the next sampling period. Therefore, a delay of one sampling period will occur. When the frequency of the command signal is comparatively low in three-phase inverters, STATCOMs and PWM rectifiers, the tracking error is very small and may be neglected. However, the frequency of the harmonic current compensated by the APFs is comparatively high. If the delay is not remedied, the delay of one sampling and calculation period will seriously affect the filter effect of this APF. Therefore, the delay of one sampling period must be remedied.

The authors of [22] present a multiple synchronous rotating reference frame PI controller for active filters. Based on this feature, the preselected undesired harmonic currents are independently compensated with PI regulators in multiple synchronous reference frames. The limitation of this method consists of the significant computational burden arising from the need for multiple synchronous rotating reference frames. Moreover the number of reference frames will be doubled under unbalanced conditions. In [23], a PIS control method based on adding an S (sine) regulator to a conventional PI regulator was presented for APF applications. The control method includes seven S regulators having different resonant frequencies. Each of the resonant frequencies is tuned to the fundamental, 5th, 7th, 11th, 13th, 17th, and 19th harmonics. An experiment carried out using a 1-kVA APF prototype indicates that the control method has perfect current-tracking performance. However, this control method requires many S regulators. As a result, its structure is very complicated. Moreover, when the characteristics of the load current change and the new harmonic components are produced, the control effects of this method will deteriorate. The authors of [24] presented a fuzzy proportional-integral controller (FPIC) used to provide the appropriate switching pattern of an APF to generate the actual compensation current. However, the THDs of the compensated experimental line currents were somewhat larger and these experimental results cannot agree reasonably well with the theoretical predictions.

This paper analyzes the shortages of the conventional current state feedback decoupling PI control in detail and concludes that canceling the delay of one sampling period and remedying the misadjustment for tracking the harmonic current are the key problems of this PI control method. Then a novel PI control method is presented. In this PI control, the predictive output current value is obtained by a state observer. The delay of one sampling period in this digital control system is remedied by the state observer. The predictive harmonic command current value is obtained by a repetitive predictor synchronously. The repetitive predictor can achieve better prediction of the harmonic current. By this means, the misadjustment of the conventional PI control for tracking the harmonic current is cancelled. This PI control method has a fast dynamic convergence rate and little static misadjustment. The experiment results illustrate that the performance of the proposed approach is satisfactory.

II. Operating Principle and Control System

The operating principle of the APF is shown in Fig.1. After the load currents flow through the current transformers, the desired currents, which the APF should compensate, are first obtained by the detecting circuit of the harmonic currents. Then the desired currents are injected into the power system by the APF controlling the PWM inverter. It can be seen from Fig. 1 that the source current i_s is provided with both the load current i_l and the output current i_c of the APF, i.e., $i_s = i_l + i_c$. Since $i_c = -i_h$, the power source only supplies i_1. Hence, i_s, after compensation, becomes a sinusoidal current which has a frequency that is identical to u_s. This is the basic operating principle of the APF. The three-level NPC inverter applied to the APFs, as shown in Fig. 1, is built-up of twelve switches, each with a freewheeling diode, and six power diodes. This allows for the connection of the phase outputs to the middle voltage. The blocking voltage of each switch is 1/2 of the DC voltage. Each arm of the inverter can be clamped to the DC terminals P, N and Q, to produce three switching states.

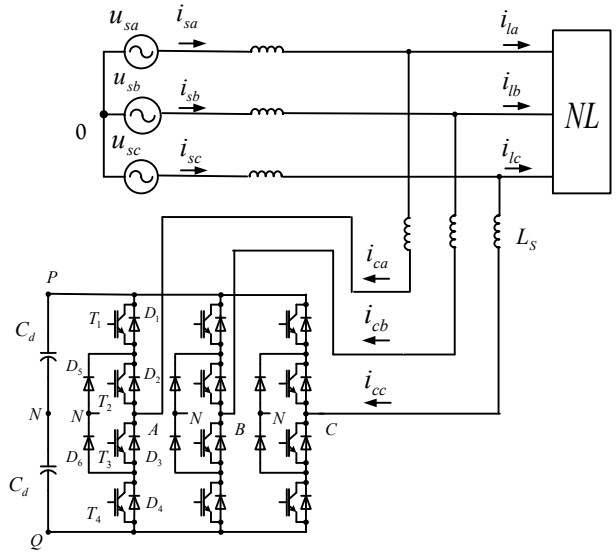

Fig. 1. Schematic diagram of the active power filter with three-level inverter.

When the upper two switches (T_1 and T_2) are switched on, the output of this phase is connected to the DC terminal P. When the middle two switches (T_2 and T_3) are switched on, the output of this phase is connected to the middle point N. Similarly when the lower two switches (T_3 and T_4) are switched on, the output of this phase is connected to Q. The allowed logic configurations of the NPC switches are able to provide the three different output voltage values furnished by each NPC inverter phase. The states of T_1, T_2, T_3 and T_4 are complementary. The two switches for each phase of the NPC inverter are closed, whilst the other two are opened at every time instant [5].

From Fig.1, the control system model for tracking the command current of the three-level APF in the stator coordinates is established as follows:

$$\begin{cases} L_s \dfrac{di_{ca}}{dt} = u_{sa} - Ri_{ca} - u_a \\ L_s \dfrac{di_{cb}}{dt} = u_{sb} - Ri_{cb} - u_b \\ L_s \dfrac{di_{cc}}{dt} = u_{sc} - Ri_{cc} - u_c \end{cases} \tag{1}$$

In this paper, the power loss on the resistor R is assumed to include all of the filter's losses. Where u_{sa} , u_{sb} and u_{sc} are the utility voltages, u_a , u_b and u_c are output voltages of the three-level inverter. Through a synchronous rotating transformation, the equation in the ABC stationary frame can be expressed in the *d-q* frame as follows:

$$\begin{cases} L_s \dfrac{di_{cd}}{dt} = u_{sd} - Ri_{cd} + \omega Li_{cq} - u_d \\ L_s \dfrac{di_{cq}}{dt} = u_{sq} - Ri_{cq} - \omega Li_{cd} - u_q \end{cases} \tag{2}$$

By this means, the three-phase alternating signal is changed into a two-phase alternating signal. Thus, the mathematic model of this APF is predigested. A diagram of the control system is shown in Fig.2. The control system includes an outer-loop voltage controller and an inner-loop current controller. The outer-loop controller is used to produce the command active current to regulate the DC voltage. The inner-loop current controller is divided into the detection module for calculating the harmonic current and the control module for tracking the command current and restraining the neutral-point voltage imbalance. In order to control the shape of the output current waveform, a novel PI control technology is presented. The neutral-point voltage imbalance is restrained by selecting the small vectors that will move the neutral-point voltage in the direction opposite the direction of the unbalance from the space vector PWM point of view in the control module [25].

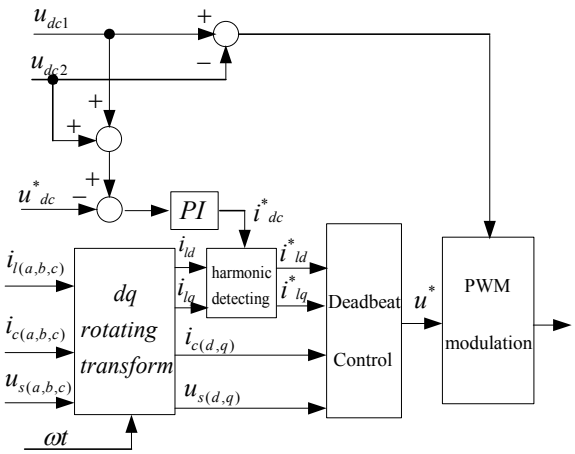

Fig. 2. Block diagram of control system of the active power filter with three-level inverter.

III. NOVEL PI CONTROL METHOD

Traditionally, the current state feedback decoupling PI control is an effective means for three-phase systems in the current control of high frequency PWM reversible rectifiers. From (2), a block diagram of the PI control system is as shown in Fig. 3 [13]-[15], [20]. Through this PI control method, the equivalent decoupling control diagrams for i_d and i_q can be derived as shown in Fig. 4. *KP* and *KI* are the proportional and integral parameters of the PI controller, respectively. The control plant is a first-order. The current control closed-loop with the PI controller is a typical second-order system.

$$C(s) = \frac{i_c(s)}{i_c^*(s)} = \frac{(K_P / L_S)s + K_I / L_S}{s^2 + [(K_P / L_S)s] / L_S + K_I / L_S} \tag{3}$$

The current control closed-loop is a typical second-order system which can be corrected by a PI controller into a first-order element by means of the Siemens method. The Siemens method is widely used in the actual tuning of the PI parameters. The core thought of this design is to let the zero

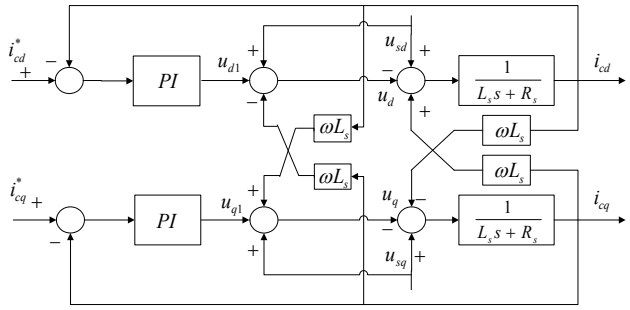

Fig. 3. Block diagram of current state feedback decoupling PI control.

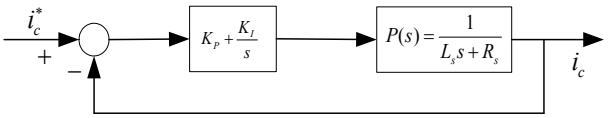

Fig. 4. Block diagram of equivalent decoupling control.

of the controller offset the pole of the plant in the *s*-plane. That is to say, $K_P / K_I = L_s / R_s$. Using this method, the PI parameter K_P and K_I are designed as follows:

$$K_P = L_s / T_s, K_I = R_s / T_s \tag{4}$$

Where T_s is sampling\switch period. Substituting equation (4) into (3) yields the following results:

$$C(s) = \frac{i_c(s)}{i_c^*(s)} = \frac{K_P}{K_P + L_S s} = \frac{1}{1 + (L_S / K_P)s} = \frac{1}{1 + T_P s} = \frac{1}{1 + T_S s} \tag{5}$$

From expressions (5), it can be seen that the closed-loop current control system is corrected into a first-order element. The time constant T_P of the closed-loop current control is equal to the switch period T_s.

The bode map of *C(s)* is as Fig. 5. From the bode map of *C(s)*, *C(s)* has a close-to-unit gain in the low frequency band. Because the fundamental signal is converted into a DC quantity through a synchronous rotating transformation, the conventional PI controller, which is designed with above-mentioned method, has little static misadjustment in the PWM reversible rectifier. However, the command currents of the APFs include a large number of harmonics. From the bode map of *C(s)*, the magnitude of *C(s)* degrades in the high and medium frequency bands. The bandwidth of this PI controller is almost enough for effectively tracking the command harmonic current. The PI controller has a static misadjustment for tracking the command current, and the system current waveform filtered has a large THD. In order to make the output current track the compensation harmonic reference well, the gain of the PI controller should be increased. However, doing that might cause oscillations and instability of the APF.

From expressions (5), the discrete equivalent equation of

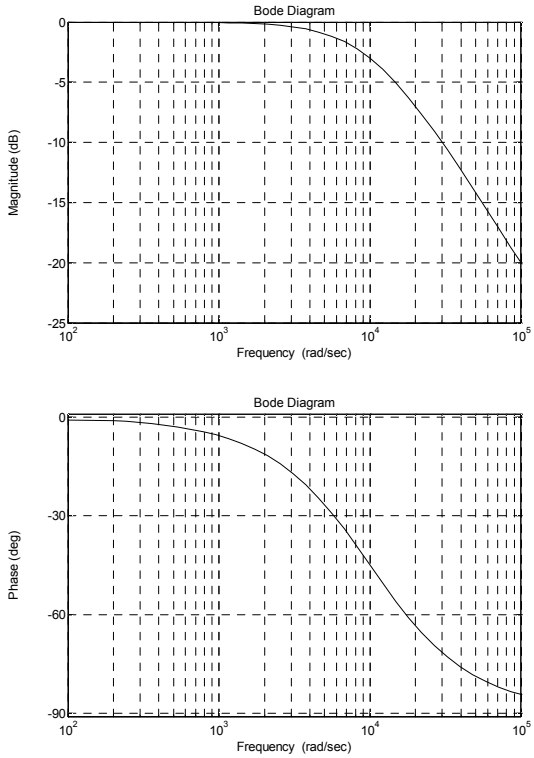

Fig. 5. bode map of *C(s)*.

the closed-loop current control system can be represented as:

$$T_s \frac{i_c(k+1) - i_c(k)}{T_s} + i_c(k) = i_c^*(k) \tag{6}$$

Simplifying expressions (6), the answer can be represented as:

$$i_c(k+1) = i_c^*(k) \tag{7}$$

From expressions (7), it can be seen that the output compensation current at the *(k+1)th* sampling instant is equal to the command harmonic current at the *kth* instant in the above-mentioned digital PI control system. Therefore, the output current lags the command current by one sampling period. Thus, the controller has a static misadjustment. If the command harmonic currents $i_c^*(k+1)$ can be predicted at the *kth* instant and $i_c^*(k+1)$ is substituted for $i_c^*(k)$ in equation (7), the following results may be obtained:

$$i_c(k+1) = i_c^*(k+1) \tag{8}$$

By this means, the misadjustment of the conventional PI control for tracking the harmonic current is cancelled. Therefore, predicting the harmonic currents at the coming sampling instant precisely is an effective method to improve this controller.

Moreover, the execution of the control program needs time. The calculation of the command voltage should be carried out a sampling period ahead, otherwise the maximum output pulse width will be significantly reduced. When the

calculation of the command voltage is carried out in the above sampling period, that is to say, the command voltage calculated in the *(k)th* sampling period is carried out in the *(k+1)th* sampling period, a delay of one sampling period will occur. The question can also be represented as:

$$i_c^*(k+1) = i_c^*(k) \tag{9}$$

If the control system follows the command current accurately, the output current of the APF can be represented as:

$$i_c(k+1) = i_c^*(k) \tag{10}$$

Expression (10) is the same as expressions (7). Therefore, the bode map of expression (10) is the same as Fig.5. The frequency of the harmonic current compensated by the APF is higher than the inverter, the STATCOM and the PWM rectifier. From the bode map in Fig.5, the delay error of one sampling period in the APF system (when the harmonic required to be compensated is 3KHz) is large. Furthermore, if the delay of one sampling and calculation period is not remedied, the delay will seriously affect the filter effect of this APF. As a result, remedying the delay of one sampling period is another key problem in improving this controller.

Therefore, the control process should be like this: at the *(k-1)th* instant, sample the output current $i_c(k-1)$ of the APF, then estimate $i_c(k)$. Meanwhile, sample the load current $i_l(k-1)$ and calculate the harmonic current $i_h(k-1)$, then predict $i_h(k+1)$. Finally the predicted value $i_h(k+1)$ is put into the PI controller of the closed-loop current control system. Using this approach, the control system can track the command current with no static misadjustment.

A good solution for the estimation of the APF output currents $i_c(k)$ is a state observer. From (2), the control system model for tracking the command current can be changed as follows:

$$\dot{X} = A \cdot X + B \cdot U \tag{11}$$

$$X = \begin{bmatrix} i_{cd} & i_{cq} \end{bmatrix}^T \qquad U = \begin{bmatrix} u_{sd} - u_d & u_{sq} - u_q \end{bmatrix}^T$$

$$A = \begin{bmatrix} -\frac{R_s}{L_s} & \omega \\ -\omega & -\frac{R_s}{L_s} \end{bmatrix} \qquad B = \begin{bmatrix} \frac{1}{L_s} & 0 \\ 0 & \frac{1}{L_s} \end{bmatrix}$$

Then the sample data model becomes as follows:

$$X(k+1) = G \cdot X(k) + H \cdot U(k) \tag{12}$$

$$X(k) = \begin{bmatrix} i_{cd}(k) & i_{cq}(k) \end{bmatrix}^T$$

$$U(k) = \begin{bmatrix} u_{sd}(k) - u_d(k) & u_{sq}(k) - u_q(k) \end{bmatrix}^T$$

$$G = e^{A \cdot T_s} \qquad H = (e^{A \cdot T_s} - I) \bullet A^{-1} \bullet B$$

A full order state observer for this APF is as follows:

$$\hat{X}(k+1) = G \cdot \hat{X}(k) + H \cdot U(k) + T(X(k) - \hat{X}(k)) \tag{13}$$

Where T is the observer gain. The state predictor is as Fig.6. $\hat{X}(k)$ and $\hat{X}(k+1)$ denote the estimated values of the output currents at the *kth* and *(k+1)th* sampling instants.

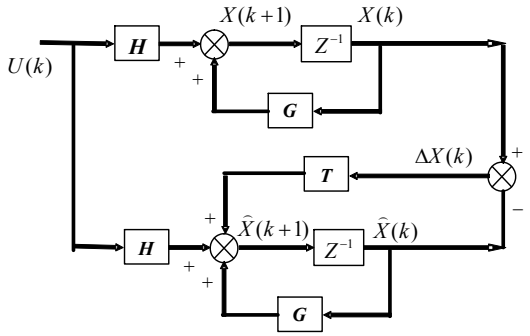

Fig. 6. The state predictor.

The observer gain is decided so that a stable pole placement is realized in the observer.

From (12) and (13), the error system is:

$$e_x(k+1) = (G - T) \cdot e_x(k) \tag{14}$$

Where $e_x(k+1) = X(k) - \hat{X}(k)$ is the observer error. The poles of the observer can be arbitrarily placed by adjusting the feedback gain T. In practice, it is easy to make the observer error quite close to zero by setting the poles of the observer suitably.

It seems impossible to model the load current disturbance precisely when considering the diversity of load types. Since the harmonic is repetitive most of the time, it makes sense to adopt a repetitive algorithm to predict the seemingly unpredictable load currents [20]. The basic theorem of the repetitive harmonic predictor is show as Fig.7.

The algorithm can be seen as a plug-in repetitive compensator for a basic predictor. The basic predictor is a unit delay: z^{-2}, which means that it just takes the value of harmonic current at the *kth* sampling instant (namely $i_{hd}(k)$, $i_{hq}(k)$) for the harmonic current values at the *(k+2)th* sampling instant since the *(k+2)th* sampling process has not yet begun. The input of the compensator is *e,* which is defined as the difference between the value of the actual current and the estimated value. It is assumed that harmonic current is sampled N times in a fundamental cycle. In order to repetitively compensate the error of the basic prediction, N memory cells are prepared to store the correction values (namely $\triangle(k)$, $k \in [1,N]$) in one fundamental cycle. The predicted value of the harmonic current at the *(k+2)th* sampling instant (namely $\hat{i}_h(k+2)$) can be obtained by adding $\triangle(k)$ to the value of the harmonic current at the *kth* sampling instant, as (13). The correction value $\triangle(k)$ for correcting the basic prediction value $i_h(k)$ to predict $\hat{i}_h(k+2)$ is modified periodically by adding the prediction error to the current correction value $\triangle(k)$. The prediction error is obtained by subtracting the predicted value of the harmonic current $\hat{i}_h(k+2)$ from the actual harmonic current value $i_h(k+2)$.

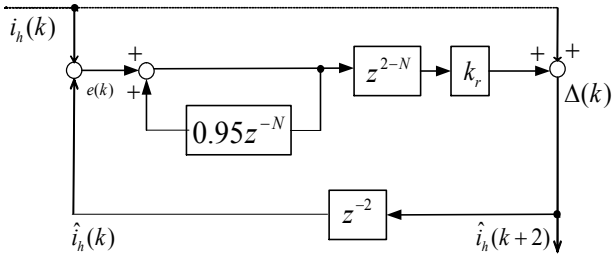

Fig. 7. The repetitive predictor.

$$\hat{i}_h(k+2) = i_h(k) + \Delta(k) \tag{15}$$

Due to the unperfected modeling, a bandlimit filter is often included in a repetitive controller. Such a filter can improve the stability of the filter system by eliminating the error *e* by half. This filter equals 0.95 (the parameter was shown to be suitable in most of our simulations). In this case, the basic estimator is just a simple and fixed algorithm, and not a real physical system where measuring errors and parameter drift are inevitable. As for the gain k_r, when it is set to be unity, the error will be compensated nearly 100% in the second cycle under a repetitive input. However, in practice, the load current does not exactly repeat itself from cycle to cycle. For a smooth convergence of the error, k_r should be chosen as less than 1. The simulation results show that the value k_r =0.98 appear to be a good choice for all of the experiments.

IV. EXPERIMENTAL RESULTS

The experimental parameters are shown as follows. The nonlinear load is a three-phase bridge rectifier with inductance and resistance. The source RMS phase voltage value is 110V and the power frequency is 50Hz. The impedance of the voltage source is 1mH. The filter inductance is 2mH and the resistor of the APF output filter is 0.5Ω. The DC voltage of the filter is 360V and the DC capacitor of the filter is 4700μF. Both the sampling frequency of the control system and the switch frequency of the switching device are 9.6kHz. The DC controller parameter kp is 1.6 and kI is 64. Repetitive predictor parameter kr is 0.98. A P-MOSFET 2SK1020 is selected as the switching device. Some important experimental oscillograms are shown as follows:

Fig. 8 shows the waveforms of both the load and utility current through the APF filtering. Waveform 2 is the utility current and waveform 1 is the load current with the help of the harmonic compensation of the three-level APF with the new PI controller. It can be calculated from these figures that the value of the total harmonic distortion (THD) can be reduced from 22.54% to 3.3%. Fig.9 shows the waveforms of both the load and utility current through the APF filtering with the traditional PI controller. The THD value of the utility current can be calculated as 6.1%. Obviously, the

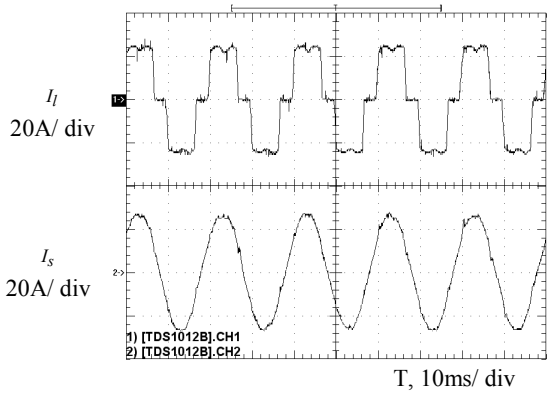

Fig. 8. Experimental steady waveforms of load current and system supply current.

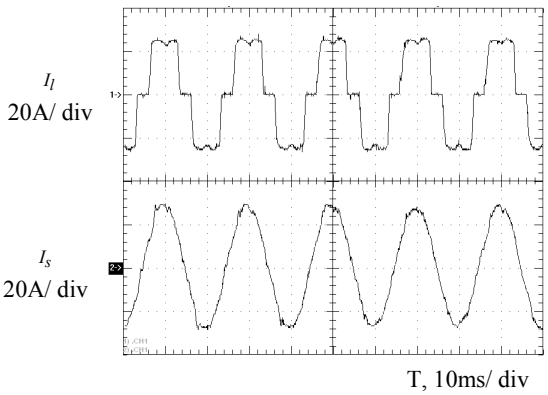

Fig. 9. Experimental steady waveforms of load current and system supply current with this traditional PI controller.

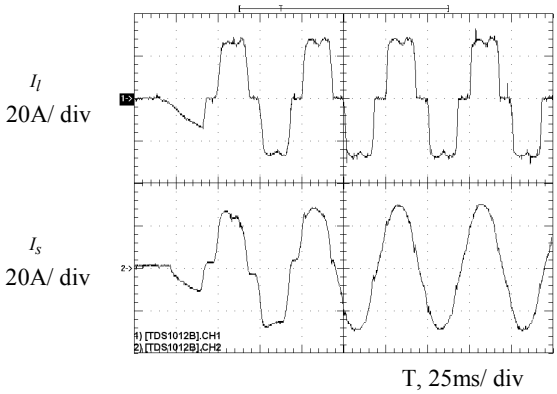

Fig. 10. Experimental dynamic waveforms of load current and system supply current when nonlinear load is added abruptly.

filtering ability of this new PI controller is better than the traditional PI controller. Fig.8-9 prove that the new proposed PI controller has good steady filtering capability.

In order to test the dynamic response characteristic of this PI controller, some of the dynamic waveforms were recorded when load switched on and off, as shown in Fig.10~11 respectively. As shown in Fig.10, from waveform 2, it can be seen that the composite controller responds to the current reference very quickly. When the load is switched on

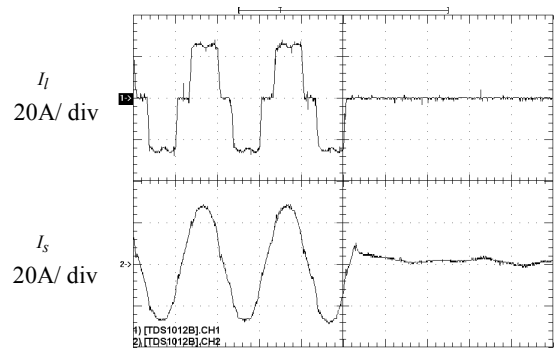

Fig. 11. Experimental dynamic waveforms of load current and system supply current when nonlinear load is removed abruptly.

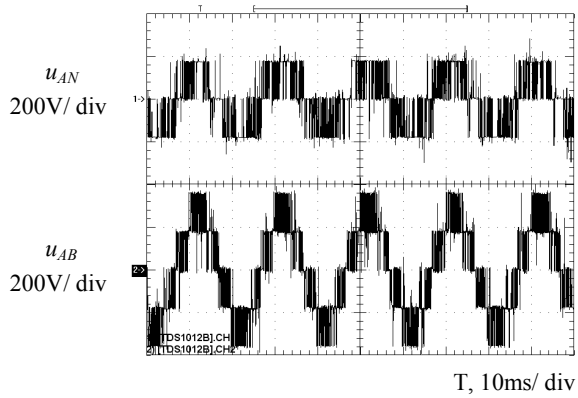

Fig. 12. Experimental waveforms of u_{AN} and u_{AB}.

suddenly, the reference distortion lasts only two periods. In Fig.11, waveform 2 shows the output current of the APF when the load is switched off. The PI controller also responses very quickly. It is obvious that the proposed APF is controlled very well by the PI control.

The experimental waveforms of u_{AN} and u_{AB} are illustrated in Fig.12, where waveform 1 is u_{AN} and waveform 2 is u_{AB}. It is obvious that the output voltage u_{AN} furnished by each NPC inverter phase is three-level and that the line-line output voltage u_{AB} is five-level. Fig.12 shows that the proposed APF is suitable for the application field of voltage grids ranging from 600V to 1000V.

V. CONCLUSIONS

Based on a detailed performance analysis of the traditional current state feedback decoupling PI control for APFs, this paper proposed a novel PI controller to improve the steady state compensation precision and ensure the dynamic response performance. This novel PI control algorithm can suppress the periodic error in the whole system to achieve zero steady error tracking. The feasibility of this control method is verified by theoretical analysis and laboratory tests.

ACKNOWLEDGMENT

This work was supported by Innovation Foundation of State Key Laboratory of Electrical Insulation and Power Equipment (No.EIPE13307), Delta Educational Development Foundation (DREG2013007) and with grants from National High Technology Research and Development Program of China (2012AA050206) and National Science Foundation of China (No.50907052).

REFERENCES

[1] P. Kumar and A. Mahajan, "Soft computing techniques for the control of an active power filter," *IEEE Trans. Power Del.,* Vol. 24, No. 1, pp. 452- 461, Jan. 2009.

[2] H. A. Ramos-Carranza, A. Medina and G. W. Chang, "Real-Time Shunt Active Power Filter Compensation," *IEEE Trans. Power Del.,* Vol. 23, No. 4, pp. 2623-2625, Oct. 2008.

[3] B. Singh and V. Verma, "Selective compensation of power-quality problems through active power filter by current decomposition," *IEEE Trans. Power Del.,* Vol. 23, No. 2, pp. 792-799, Apr. 2008.

[4] S. Hirve, K. Chatterjee, B. G. Fernandes, M. Imayavaramban, and S. Dwari, "PLL-Less Active Power Filter Based on One-Cycle Control for Compensating Unbalanced Loads in Three-Phase Four-Wire System," *IEEE Trans. Power Del.,* Vol. 22, No. 4, pp. 2457-2465, Oct. 2007.

[5] N. Akira, I. Takahashi, and H. Akagi, "A new neutral-point-clamped PWM inverter," *IEEE Trans. Ind. Applicat.,* Vol. 17, No. 3, pp. 518-523, Sep. 2007.

[6] H. Akagi and R. Kondo, "A transformerless hybrid active filter using a three-level PWM converter for a medium-voltage motor drive," *in Proc. ECCE,* pp. 1732 -1739, 2009.

[7] H. Akagi and T. Hatada, "Voltage Balancing Control for a Three-Level Diode-Clamped Converter in a Medium-Voltage Transformerless Hybrid Active Filter," *IEEE Trans. Power Del.,* Vol. 24, No. 3, pp. 571-579, Mar. 2009.

[8] H. Rudnick, J. Dixon, and L. Moran, "Delivering clean and pure power," *IEEE Power and Energy Magazine.* Vol. 1, No. 5, pp. 32-40, Sep./Oct. 2003.

[9] M. C. Wong, J. Tang, and Y. D. Han, "Cylindrical coordinate control of 3-D PWM technology in 3-phase 4-wire tri-level inverter," *IEEE Trans. Power Electron.,* Vol. 18, No. 1, pp. 208 -220, Jan. 2003.

[10] N. Y. Dai, M. C. Wong, and Y. D. Han, "Application of a three-level NPC inverter as a three-phase four-wire power quality compensator by generalized 3DSVM," *IEEE Trans. Power Electron.,* Vol. 21, No. 2, pp. 440 - 449, Mar. 2006.

[11] M. Basu, S. P. Das, and G. K. Dubey, "Parallel converter scheme for high-power active power filters," *IEE Proceedings Electric Power Applications*, Vol. 151, No. 4, pp. 460-466, Jul. 2004.

[12] O. Vodyakho and C. C. Mi, "Three-level inverter-based shunt active power filter in three-phase three-wire and four-wire systems,"*IEEE Trans. Power Electron.,* Vol. 24, No. 5, pp. 1350-1363, May 2009.

[13] H. Akagi, S. Inoue, and T. Yoshii,"Control and performance of a transformerless cascade PWM STATCOM with star

configuration," *IEEE Trans. Ind. Applicat.,* Vol. 43, No.4, pp.1041-1049, Jul./Aug. 2007.

[14] L. Maharjan, S. Inoue, and H. Akagi, "A transformerless energy storage system based on a cascade multilevel PWM converter with star configuration," *IEEE Trans. Ind. Applicat.,* Vol. 44, No. 5, pp. 1621-1630, Sep./Oct. 2008.

[15] H. Akagi, H. Fujita, S. Yonetani, and Y. Kondo, "A 6.6-kV transformerless STATCOM based on a five-level diode-clamped PWM converter: System design and experimentation of a 200-V 10-kVA laboratory model," *IEEE Trans. Ind. Applicat.,* Vol. 44, No. 2, pp. 672-680, Oct. 2008.

[16] Z. Zhou, P. J. Unsworth, P. M. Holland, and P. Igic, "Design and analysis of a feedforward control scheme for a three-phase voltage source pulse width modulation rectifier using sensorless load current signal," *IET Proceedings Power Electronics,* Vol. 2, No. 4, pp. 421- 430, Jul. 2009.

[17] K. Lee, T. M. Jahns, T. A. Lipo, V. Blasko, and R. D. Lorenz, "Observer-based control methods for combined source-voltage harmonics and unbalance disturbances in PWM voltage-source converters," *IEEE Trans. Ind. Applicat.,* Vol. 45, No. 6, pp. 2010-2021, Nov./Dec. 2009.

[18] A. Yoo and S. K. Sul, "Design of flux observer robust to interior permanent-magnet synchronous motor flux variation," *IEEE Trans. Ind. Applicat.,* Vol. 45, No. 5, pp. 1670-1677, Sep./Oct. 2009.

[19] H. Fujita, "A single-phase active filter using an h-bridge PWM converter with a sampling frequency quadruple of the switching frequency," *IEEE Trans. Power Electron.,* Vol. 24, No. 4, pp. 934-941, Jun. 2009.

[20] K. Zhang, Y. Kang, J. Xiong, and J. Chen, "Deadbeat control of PWM inverter with repetitive disturbance prediction," *in Proc. APEC,* pp. 1026-1031, 1999.

[21] O. Vodyakho, D. Hackstein, A. Steimel, and T. Kim, "Novel direct current-space-vector control for shunt active power filters based on the three-level inverter," *IEEE Trans. Power Electron.,* Vol. 23, No. 4, pp. 1668-1678, Feb. 2008.

[22] M. Bojrup, P. Karlsson, M. Alakula, and L. Gertmar, "A multiple rotating integrator controller for active filters," *in Proc. EPE.,* pp. 756 -762, 1999.

[23] S. Fukuda and R. Imamura. "Application of a sinusoidal internal model to current control of three-phase utility-interface converters," *IEEE Trans. Ind. Electron.,* Vol.50, No. 2, pp. 420-426, Apr. 2005.

[24] P. Kirawanich and R. M. O'Connell, "Fuzzy logic control of an active power line conditioner," *IEEE Trans. Power Electron.,* Vol. 19, No. 6, pp. 1574-1585, Nov. 2004.

[25] N. Celanovic and D. Voroyevich, "A comprehensive study of neutral-point voltage balancing problem in three-level neutral-point-clamped voltage source PWM inverters," *IEEE Trans. Power Electron.,* Vol. 15, No. 2, pp. 242-249, Mar. 2000.

Yingjie He was born in Henan Province, China, in 1978. He received his B.S., M.S. and Ph.D. from the Huazhong University of Science and Technology, Wuhan, China, in 1999, 2003 and 2007, respectively. From May 2007 to May 2009, he was with the Power Electronics and Renewable Energy Center at Xi'an Jiaotong University, Xi'an, China, as a Postdoctoral Research Scholar. He is currently a Lecturer at Xi'an Jiaotong University. His current research interests include power quality control, multilevel inverters and the application of power electronics in power systems.

Jinjun Liu was born in Hunan Province, China, in 1970. He received his B.S. and Ph.D. from Xi'an Jiaotong University (XJTU), Xi'an, China, in 1992 and 1997, respectively. In 1998, he led the founding of the XJTU/Rockwell Automation Laboratory. From December 1999 to February 2002, he was with the Center for Power Electronics Systems at the Virginia Polytechnic Institute and State University, Blacksburg, VA, USA, as a Postdoctoral Research Scholar. After that he came back to XJTU and in August of 2002 was promoted to Full Professor and Head of the Power Electronics and Renewable Energy Center. He is also serving as an Associate Dean in the School of Electrical Engineering at XJTU. He has coauthored 3 books, published over 100 technical papers, and received several provincial or ministerial awards for scientific and career achievements. He was also a recipient of the 2006 Delta Scholar Award. His current research interests include power quality control, renewable energy generation, utility applications of power electronics, and the modeling and control of power electronic systems. Dr. Liu has served as the IEEE Power Electronics Society Region 10 Liaison for 3 years. He was actively involved in the organization of several power electronic international conferences, including PESC, APEC, IPEC in Japan, ICPE in Korea, and IPEMC in China, where he served as a Committee Member, a Co-Chair, or a Session Chair.

Zhaoan Wang was born in Shaanxi Province, China, in 1945. He received his B.S. and M.S. from Xi'an Jiaotong University, Xi'an, China, in 1970 and 1982, respectively, and his Ph.D. from Osaka University, Osaka, Japan, in 1989. From 1970 to 1979, he was an Engineer at the Xi'an Rectifier Factory, Xi'an, China. He is now a Professor at Xi'an Jiaotong University. His current research interests include power conversion systems, harmonics suppression, reactive power compensation and active power filters.

Yunping Zou was born in Hunan Province, China, in 1945. He received his B.S. from the Huazhong University of Science and Technology, Wuhan, China, in 1969. He has been a Full Professor at the Huazhong University of Science and Technology since 1994. His current research interests include new power electronic circuits, devices and systems; digital intelligent control technology and its basic application; and signal detection, transforming and processing.